# **Subnanosecond Optical Free-Induction Decay**

A novel form of laser frequency switching is devised that extends coherent optical transient studies to a 100-picosecond time scale, the measurements being performed in real time. Free-induction decay (FID) on a subnanosecond time scale reveals new features, such as a first-order FID that dephases with the inhomogeneous dephasing time  $T_2^*$  and interferes with the well-known nonlinear FID. A complete analytical expression for optical FID is derived and supports our FID observations for the sodium  $D_1$  transition.

#### Introduction

Coherent optical transient phenomena, such as the freeinduction decay (FID) effect, have been detected recently on a 100-picosecond time scale by using a novel form of laser frequency switching [1]. This development represents a fiftyfold improvement in temporal resolution over our initial version [2] of laser frequency switching which incorporated an intracavity electro-optic phase modulator. The present device is a traveling wave electro-optic phase modulator that is external to the laser cavity; the earlier advantages are still preserved, namely heterodyne detection, high sensitivity, and the ability to monitor the entire class of coherent optical transients by preselecting the voltage pulse sequence. Hence, quantitative coherent transient measurements in this time domain are now feasible.

New aspects of optical coherence become evident as the time scale is reduced. This article explores additional properties of optical FID that are noticeable in the subnanosecond region for the sodium D line transitions. Our observations confirm a complete density matrix solution of the Schrödinger wave equation, which we consider first.

#### Theory

A general expression for optical FID is presented here along with its physical interpretation; the detailed derivation will appear elsewhere [3]. Theoretically, the appearance or nonappearance of first-order FID depends on the

manner in which the optically induced dipole is averaged over the atomic velocity distribution. In earlier theories [4–6] where the laser frequency or Stark switching was assumed to be small compared to the Doppler broadening, the Gaussian lineshape was assumed to be constant over the region of integration, and therefore could be factored outside the Doppler integral. Foster, Stenholm, and Brewer [6] first predicted a rapid transient arising from the entire inhomogeneous line by retaining the Gaussian in the integral and evaluating the result approximately. Indeed, an exact analytical evaluation of their Eq. (10) forms the basis of this work where we adopt the same notation.

Let us write down Eq. (10) of Foster, Stenholm, and Brewer and examine the consequences of an analytical evaluation of the Doppler integral. Here  $\hat{\rho}_{12}$  is the familiar off-diagonal density matrix element of the transition levels 1 and 2, expressed in a frame rotating at the preparative laser frequency  $\Omega$ . The Doppler-averaged density matrix element is given by

$$\begin{split} \langle \hat{\rho}_{12}(t) \rangle &= \frac{1}{u\pi^{1/2}} \int_{-\infty}^{+\infty} \hat{\rho}_{12}(v_z, t) \, \exp\left(-v_z^2/u^2\right) dv_z \\ &= \frac{i\chi}{2\pi^{1/2}u} \, \Delta \rho_{21}^0 \exp\left(-\frac{t}{T_2}\right) \int_{-\infty}^{+\infty} \frac{i\Delta(v_z) + \gamma}{\Delta^2(v_z) + \Gamma^2} \\ &\times \exp\left[i\Delta(v_z)t\right] \exp\left(-\frac{v_z^2}{u^2}\right) dv_z, \end{split} \tag{1}$$

Copyright 1979 by International Business Machines Corporation. Copying is permitted without payment of royalty provided that (1) each reproduction is done without alteration and (2) the *Journal* reference and IBM copyright notice are included on the first page. The title and abstract may be used without further permission in computer-based and other information-service systems. Permission to *republish* other excerpts should be obtained from the Editor.

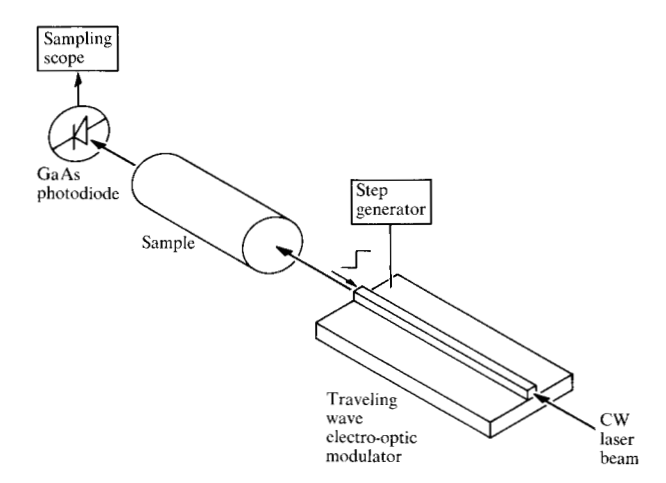


Figure 1 Schematic of the optical layout for detecting subnanosecond coherent optical transients with a traveling wave electro-optic phase modulator. The microwave guide is greatly simplified to show the crystal element (the focusing and collimating lenses to either side of it are not shown).

where the tuning parameter  $\Delta(v_z) = -\Omega + \omega_{21} - kv_z$ , the power-broadened homogeneous linewidth  $\Gamma = (1/T_2^2 + \chi^2 T_1/T_2)^{1/2}$ , the Doppler width  $\sigma = ku$  (u = velocity),  $\gamma = 1/T_2$ , the Rabi frequency  $\chi = \mu_{ij} E/\hbar$ , and  $\Delta \rho_{21}^0$  is the level population difference in the absence of excitation. This integral is just the convolution of the Lorentzian susceptibility of each velocity group with the Gaussian velocity distribution. The phase factor  $\exp\left[i\Delta(v_z)t\right]$  corresponds to the free transient decay of each velocity group; i.e., regardless of the excitation frequency, each velocity group decays at its own free resonant frequency.

We change the variable of integration from  $v_z$  to  $x \equiv \Delta(v_z)$  and define

$$\delta \equiv \omega_{21} - \Omega.$$

Then the integral (I) in Eq. (1) becomes

$$I = \int_{-\infty}^{+\infty} \frac{ix + \gamma}{x^2 + \Gamma^2} \exp(ixt) \exp\left[-\frac{(x - \delta)^2}{\sigma^2}\right] dx.$$
 (2)

This integral can be expressed analytically in terms of the error function W(z) of complex argument [7, 8], taking the form for  $t < 2\Gamma/\sigma^2$ ,

$$I = \frac{\pi}{2} \exp\left[-\left(\frac{\sigma t}{2}\right)^{2}\right] \exp\left(i\delta t\right)$$

$$\times \left\{ (\eta + 1)W\left[\frac{\delta}{\sigma} + i\left(\frac{\sigma t}{2} + \frac{\Gamma}{\sigma}\right)\right] + (\eta - 1)W\left[-\frac{\delta}{\sigma} + i\left(\frac{\Gamma}{\sigma} - \frac{\sigma t}{2}\right)\right]\right\}. \tag{3a}$$

For  $t > 2\Gamma/\sigma^2$ .

$$I = \pi(\eta - 1) \exp\left[-\left(\frac{i\Gamma - \delta}{\sigma}\right)^{2}\right] \exp\left(-\Gamma t\right)$$

$$+ \frac{\pi}{2} \exp\left[-\left(\frac{\sigma t}{2}\right)^{2}\right] \exp\left(i\delta t\right) \left[(\eta + 1)W\left(\frac{i\sigma t}{2} + \frac{i\Gamma + \delta}{\sigma}\right)\right]$$

$$- (\eta - 1)W\left(\frac{i\sigma t}{2} + \frac{-i\Gamma + \delta}{\sigma}\right), \tag{3b}$$

where the saturation parameter

$$\eta \equiv \gamma/\Gamma$$
.

It then follows in a sample of length L and atomic number density N that the FID heterodyne beat signal [9] is

$$E_{b}^{2} = K \exp(-t/T_{2}) \exp[i(\Omega - \Omega')t] \times \begin{cases} I = \text{Eq. (3a), } t < 2\Gamma/\sigma^{2} \\ I = \text{Eq. (3b), } t > 2\Gamma/\sigma^{2} \end{cases} + \text{c.c.,}$$
(4)

where

$$K = \frac{\pi^{1/2}}{2u} \hbar N L \chi^2 \Delta \rho_{21}^0.$$

This general expression reduces to the limiting cases which follow.

Long time limit For decay times longer than the inverse Doppler width such that  $\sigma t >> 1$ , we may use the asymptotic form [7] of the error function

$$W(z) = \frac{i}{\pi^{1/2}z} + \cdots \qquad z \to \infty,$$

and Eq. (4) yields a heterodyne beat signal

$$E_{\rm b}^{2}(t) = K\pi(\eta - 1) \exp\left[-(1/T_{2} + \Gamma)t\right] \exp\left[i(\Omega - \Omega')t\right]$$

$$\times \exp\left[-\left(\frac{i\Gamma - \delta}{\sigma}\right)^{2}\right] + \text{c.c.}, \tag{5}$$

where  $\sigma t >> 1 > 2\Gamma/\sigma$ . The imaginary part of the term  $\exp \{-\left[(i\Gamma - \delta)/\sigma\right]^2\}$  introduces a small phase shift in  $E_b^2$  for  $\Gamma/\sigma << 1$  and therefore makes  $E_b^2$  slightly dispersive. However, we neglect it here and obtain

$$E_{b}^{2}(t) = 2K\pi(\eta - 1) \exp\left[-\left(1/T_{2} + \Gamma\right)t\right]$$

$$\times \exp\left[-\left(\delta/\sigma\right)^{2}\right] \cos\left(\Omega - \Omega'\right)t. \tag{6}$$

This result is identical to earlier approximate derivations [4-6] where the Gaussian was factored outside the Doppler integral. We shall refer to Eq. (6) as the nonlinear FID signal since  $E_{\rm b}^2 \propto \chi^4$  at low light intensities when  $\chi^2 T_1 T_2 << 1$ . As has already been verified by experiment [4, 6, 9], the long time limit of FID displays the properties predicted by (6). First, the sample radiates at the initial laser frequency  $\Omega$  and produces a heterodyne beat signal

of frequency  $\Omega-\Omega'$  that is absorptive, and second, it decays at the rate  $1/T_2+\Gamma$  due to the preparative and postpreparative stages.

Short time limit For short times, we retain the first two terms of the power series expansion [7]

$$W(z) = \sum_{n=0}^{\infty} \frac{(iz)^n}{\Gamma(\frac{n}{2} + 1)}$$
$$= 1 + \frac{2iz}{\pi^{1/2}} + \cdots, \qquad |z| < 1.$$

In addition to the condition

$$|z| = \left| i \left( \frac{\Gamma}{\sigma} \pm \frac{\sigma t}{2} \right) \pm \frac{\delta}{\sigma} \right| < 1,$$
 (7)

we require that

$$t << 2\Gamma/\sigma^2$$

thereby allowing the  $\sigma t/2$  term to be dropped in (7). With these conditions, Eq. (4) reduces to

$$\begin{split} E_{\rm b}^2 &= 2K\pi \, \exp\left(-t/T_2\right) \, \exp\left[-(\sigma t/2)^2\right] \\ &\times \left[\gamma \left(\frac{1}{\Gamma} - \frac{2}{\pi^{1/2}\sigma}\right) \cos\left(\omega_{21} - \Omega'\right)t \right. \\ &\left. - \left(\frac{2}{\pi^{1/2}}\right) \frac{(\omega_{21} - \Omega)}{\sigma} \sin\left(\omega_{21} - \Omega'\right)t\right]. \end{split} \tag{8}$$

We refer to (8) as the first-order FID since  $E_b^2 \propto \chi^2$ . Furthermore, the decay is now Gaussian,  $\exp[-(\sigma t/2)^2]$ , where the characteristic dephasing time  $T_2^* = 2/\sigma$ . This signal contains both absorptive and dispersive parts that depend on the initial laser frequency through the factor  $(\omega_{21} - \Omega)/\sigma$ . From (8), it is evident that the atomic sample radiates at the Doppler peak  $\omega_{21}$ , independent of the initial laser frequency  $\Omega$ , and produces a heterodyne beat of frequency  $\omega_{21} - \Omega'$ . We conclude, therefore, that in the firstorder FID the various velocity packets destructively interfere, except at Doppler line center. By contrast, the nonlinear FID radiates at the initial laser frequency and therefore possesses memory of its preparation. We view these two forms of FID as the transient analogues of steady state linear and nonlinear (hole burning) laser spectroscopy of an inhomogeneously broadened transition.

Limit of no inhomogeneous broadening. In the limit  $\sigma \to 0$ , the Doppler integral for  $\langle \tilde{\rho}_{12}(t) \rangle$ , Eq. (1), must reduce to a form identical to  $\tilde{\rho}_{12}(v_z=0,t)$ , thus checking our calculation. As  $\sigma \to 0$ ,  $2\Gamma/\sigma^2 \to \infty$ , so the short time form of the integral must be used. The argument of the W(z) function approaches  $z=(\pm\delta+i\Gamma)/\sigma$  and its modulus approaches infinity as  $\sigma \to 0$ , so we may again use the asymptotic form

$$W(z) = \frac{i}{z^{1/2}z} + \cdots, \qquad |z| \to \infty, \operatorname{Im}(z) > 0.$$

In this limit.

$$\begin{split} E_{\rm b}^2 &= \frac{2K\sigma\pi^{1/2}}{\Gamma^2 + \delta^2} \exp\left(-\frac{t}{T_2}\right) \\ &\times \left[\gamma \cos\left(\omega_{21} - \Omega'\right)t - \delta \sin\left(\omega_{21} - \Omega'\right)t\right], \end{split} \tag{9} \\ \text{where } \delta &= \omega_{21} - \Omega \text{ and } K\sigma = (\pi^{1/2}/2) \, k\hbar NL\chi^2 \Delta \rho_{21}^0. \end{split}$$

As expected, Eq. (9) can be derived [9] directly from  $\hat{\rho}_{12}(t)$  without Doppler averaging when  $v_z=0$ . The radiation now occurs at the atomic transition frequency  $\omega_{21}$  regardless of the laser excitation frequency  $\Omega$ , with an amplitude, frequency, and relaxation dependence identical to that of  $\hat{\rho}_{12}(v_z=0,t)$ . The FID again exhibits a linear intensity dependence. Equation (9) also agrees with the well-known FID theory of nuclear magnetic resonance [10].

## Experimental technique

### • Traveling wave modulator

To study subnanosecond coherent transients by laser frequency switching, new techniques are required. At such speeds, it is no longer advantageous to place the electro-optic modulator inside the laser cavity as in the past [2], since the transient dies away before the laser beam completes one round trip through the optical cavity. On the other hand, when the modulator is external to the laser cavity, the modulator design can be varied easily while still retaining the advantages of undiminished laser intensity and stability. A novel traveling wave electro-optic modulator that permits such measurements is described here.

Two requirements must be satisfied in laser frequency switching to insure the generation of intense coherent transient signals. First, the laser frequency switch must exceed the homogeneous linewidth  $1/\pi T_2$ , and second, the switching time should be less than the dephasing time T<sub>a</sub>. Therefore, measurements on a subnanosecond time scale imply a shift of several gigahertz with an approximately 100-ps rise time. A schematic diagram of our apparatus is shown in Fig. 1. It consists of a stable continuous wave (cw) dye laser, a traveling wave electro-optic modulator, the sample, a fast photodiode detector, and a sampling oscilloscope. The frequency-shifted laser beam produces in the sample coherent transients which are detected in the forward direction in real time. All emission signals, such as the FID or the photon echo, appear as heterodyne beat signals, as discussed previously [4, 9].

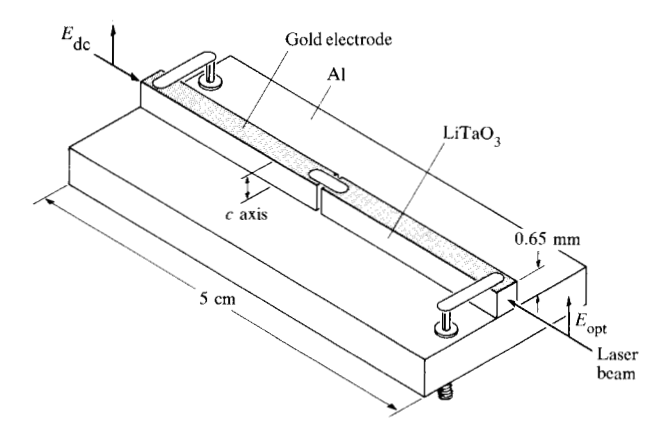


Figure 2 Detailed drawing of the LiTaO<sub>3</sub> traveling wave electro-optic modulator crystal elements mounted on an aluminum substrate of the microwave guide.

The traveling wave electro-optic modulator was invented initially by Kaminow [11] in 1961. We have used it in a new configuration. Compared to intracavity frequency switching, the rise times and frequency shifts are at least one order of magnitude more favorable. The principle of operation of our configuration is the following. An electro-optic crystal constituting an integral part of a microwave transmission line allows a cw laser beam and a direct current voltage pulse to simultaneously propagate longitudinally along one crystal axis, as shown in Fig. 2. As the dc field advances down the crystal, it produces a zone of increasing refractive index  $n_0 \rightarrow n_1$ , which shifts the phase  $\phi$  of the light wave uniformly in time and hence its angular frequency  $\Omega$  where

$$\Omega - \Omega' = \frac{d\phi}{dt} \tag{10}$$

This behavior is easily derived by noting that the phase of the light wave emerging from a crystal of length  $\ell$  at time t is

$$\phi(\ell, t) = \int_0^\ell k n(z) dz$$

$$= \int_0^{vt'} k n_1 dz + \int_{vt'}^\ell k n_0 dz,$$
(11)

where  $\vec{k}$  is the optical propagation vector and v and c are the velocities of the dc field and light wave in the crystal medium. Consider first the case of copropagating fields. If a step function dc field pulse enters the crystal at z=0 at time t=0, then at the intermediate time t' when the light wave is just at the boundary of  $n_0$  and  $n_1$ , the obvious relation

$$vt' + c(t - t') = \ell \tag{12}$$

holds. Inserting  $t' = (\ell - ct)/(v - c)$  into (11), the fre-

quency shift according to (10) is

$$\Omega - \Omega' = \Omega \frac{n_1 - n_0}{n_0} \left( \frac{v}{c \pm v} \right), \tag{13}$$

where the minus sign corresponds to copropagating fields. By a similar argument, for counterpropagating fields the plus sign follows. The singularity in (13) for v=c is artificial and results from our neglecting the pulse rise time, which is zero for the step function just mentioned. For typical values of these parameters, to be discussed, gigahertz shifts are easily accomplished, particularly in the visible or ultraviolet region due to the large factor  $\Omega \approx 10^{15}$  Hz. Of course, once the dc pulse reaches the end of the crystal  $d\phi/dt = 0$  and the frequency shift is zero.

This technique possesses several advantages over more conventional traveling wave modulators [12a]. First, conventional devices do not employ de square wave pulses and require additional microwave techniques to phase match the microwave wave velocity to the light wave velocity. This matching is never perfect and degrades the rise time of the crystal. In our design the rise time is determined primarily by the crystal connections which we believe can approach 20 ps. Second, a conventional traveling wave modulator, when driven by a dc voltage ramp where  $V(t) \propto t$ , can produce a frequency shift but it is impractical. Producing a ramp with constant slope, a sharp corner at t = 0, and no ringing appears to be a formidable task in the 100-ps region. Also, in our design, once the modulating wave is launched into the crystal, it will attenuate slowly and the frequency shift will be highly uniform.

Third, previous devices require microwave sources which generate a distribution of optical sidebands corresponding to the various microwave harmonics. Therefore, the modulation efficiency is often low. In our arrangement with dc voltage pulses, all of the light is shifted uniformly.

Fourth, as already stated, intracavity switching [2], which requires the application of a transverse field, will not satisfy our requirements either. For example, electrooptic AD\*P (ammonium dideuterium phosphate) crystals cannot be frequency-switched fast enough or far enough. The electro-optic coefficient is too low for gigahertz frequency shifts with available voltages. Furthermore, these crystals are not easily matched to a 50- $\Omega$  driver impedance, since their characteristic capacitance of  $\approx$ 40 pF implies an RC rise time of 2 ns. More importantly, the modulating voltage takes at least 500 ps to travel across the crystal. However, rather than trying to overcome the transit time problem, we have used it as the operating principle of our traveling wave modulator.

The unique features of our traveling wave modulator therefore facilitate rapid FID measurements and other coherent transient effects by a variation of the pulse sequence.

#### Apparatus

The optical phase modulator consists of two lithium tantalate crystals of dimensions  $0.5 \text{ mm} \times 0.65 \text{ mm} \times$ 25 mm, as shown in Fig. 2. The end faces are polished and anti-reflection-coated, and gold electrodes are deposited on opposite faces to form a parallel plate transmission line. A voltage between the electrodes produces an electric field parallel to the c axis. For a given applied voltage, the electric field, and hence the frequency shift, is inversely proportional to the electrode spacing. The crystal therefore is chosen to be as narrow as possible up to the optical diffraction limit. Kogelnik [13] has calculated the optimum focusing arrangement for such a case. We used a 10-cm lens which produces a 1/e field spot diameter of 150 µm at the crystal apertures. The crystal must consequently be aligned to an angle of  $\approx 1$  mrad and to a position of 50  $\mu$ m to avoid beam distortion. A second 10-cm lens recollimates the beam before it enters the sample cell.

The ratio of height to width of the crystal (0.65 mm to 0.50 mm) was chosen so that, given the microwave dielectric constant of lithium tantalate ( $\epsilon = 43$ ), the crystal appears to be a 50- $\Omega$  transmission line. The electrical rise time of the crystal and the quality of the impedance match to an external 50- $\Omega$  line were tested with a time domain reflectometer that revealed 100-ps rise times. Using the known electro-optic coefficient [12b] of lithium tantalate,  $r_{33} = 3.04 \times 10^{-9} \, \text{cm/V}$ , we calculate  $\Delta n/V = -2.43 \times 10^{-7}/V$  using standard techniques [12c]. Inserting this into Eq. (13), we obtain  $\Omega - \Omega'/2\pi = 13.9 \, \text{MHz/V}$ , which agrees with our experimental value to within 10%.

The beam from a single-mode cw dye laser (Coherent 599) passes through a focusing lens, the LiTaO $_3$  modulator crystal, a collimating lens, and a sample cell containing sodium vapor. It emerges together with the forward FID emission and is focused to a 40- $\mu$ m-diameter spot on a fast GaAs-GaAlAs photodiode (Rockwell International Corp., Thousand Oaks, CA 91360) [14]. The photodetector of 50- $\mu$ m diameter has a response time of 30 ps or less and is mounted directly on an S-4 sampling head (25-ps response) of a Tektronix 7904 oscilloscope with a 7S11 sampling unit. Because the photodiode has a low cw power rating, a Pockel's cell optical shutter blocks the laser light except for a 2- $\mu$ s interval, immediately before and after the frequency switch, so that the FID signal can be seen during this period.

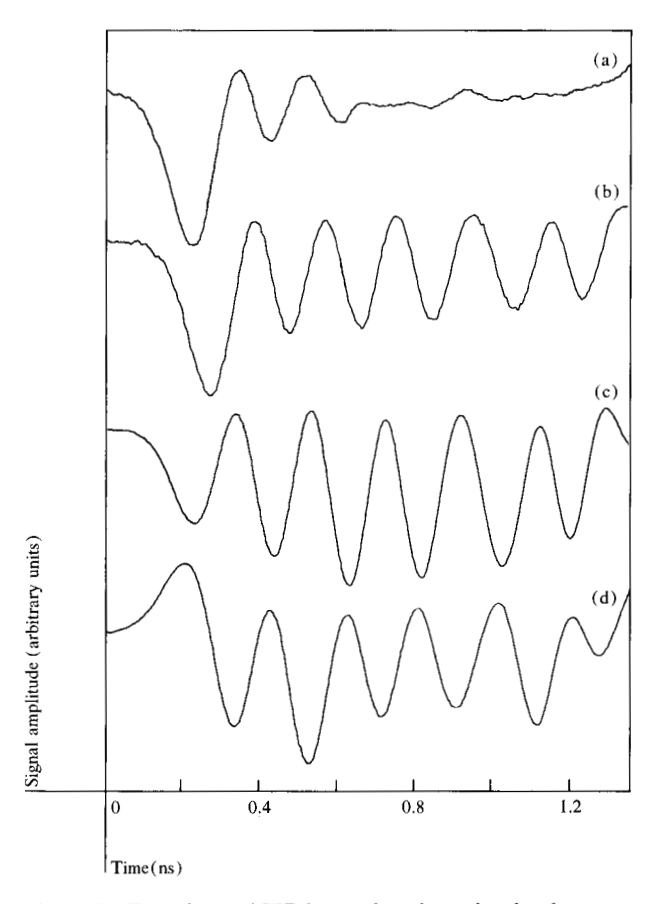


Figure 3 Experimental FID heterodyne beat signals where  $\chi=0.8$  GHz and  $\delta\equiv(\omega_{21}-\Omega)/2\pi$  in GHz equals (a) 1.5, (b) 0.7, (c) 0.0, and (d) -1.0. The laser frequency shift is  $(\Omega-\Omega')/2\pi=5$  GHz, corresponding to a 335-V dc square wave pulse. The gain in (a) is  $2\times$ .

The step function dc modulating voltage is generated at a 700-Hz repetition rate by a Tektronix 109 reed relay pulser, where the output is delayed by 75 ns to permit triggering the Pockel's cell and the 7T11 sampling time base.

#### Measurements

Coherent transients on a 100-ps time scale were detected for both  $\rm I_2$  vapor and atomic sodium. However, the large number of closely spaced hyperfine transitions in  $\rm I_2$ , which are distributed over one Doppler width, produce heavily modulated FID signals and at present are difficult to interpret. Therefore, to avoid unnecessary complications in these initial studies, experiments were performed on atomic sodium vapor, which permits a quantitative test of the above FID theory.

The transition monitored is the sodium  $D_1$  line  ${}^2P_{1/2} \leftrightarrow {}^2S_{1/2}$  at 16 956.16 cm<sup>-1</sup>. As is well known, its hyperfine

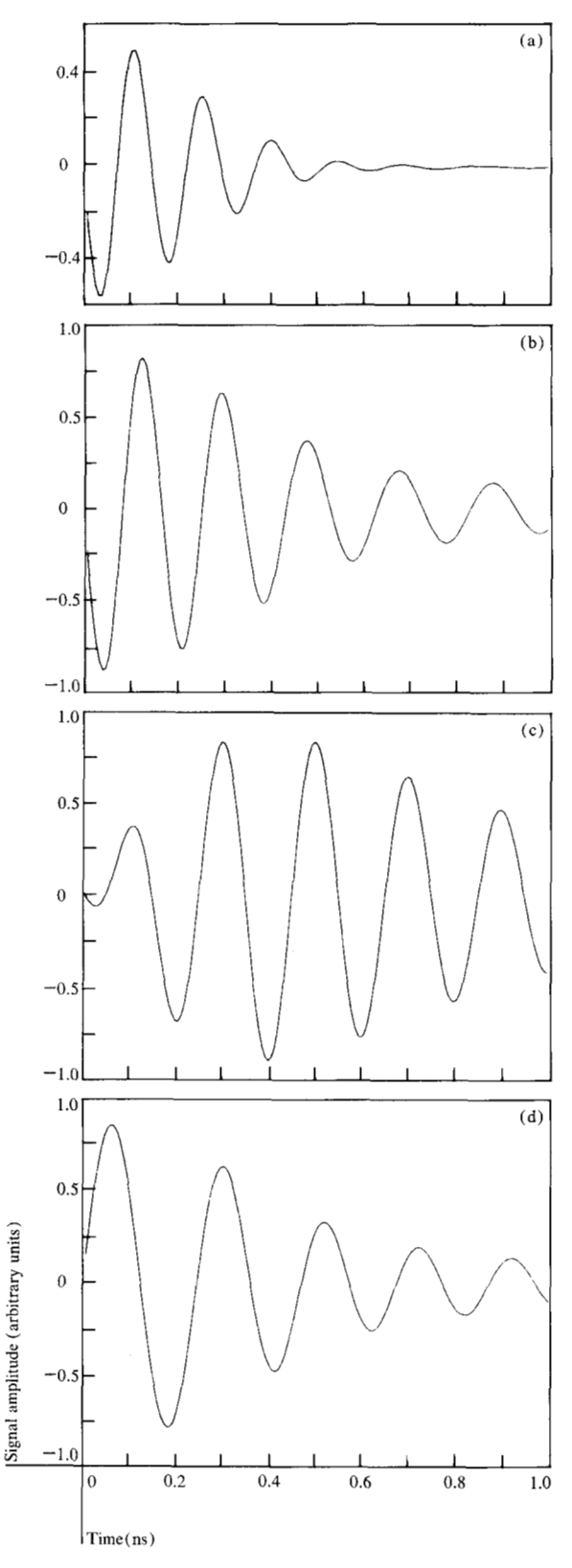


**Figure 4** Numerical solution of the FID heterodyne beat signal  $E_b^2(L, t)$  of Eq. (4), where  $\chi=2.3$  GHz,  $(\Omega-\Omega')/2\pi=5$  GHz and  $(\omega_{21}-\Omega)/2\pi$  in GHz equals (a) 1.5, (b) 1.0, (c) 0.0, and (d) -1.0.

splitting, 192 MHz ( $^{2}P_{_{1/2}}$ ) and 1.772 GHz ( $^{2}S_{_{1/2}}$ ), produces two pairs of lines. The initial laser frequency  $\Omega$  is tuned to the center of the low-frequency pair, and the traveling wave modulator voltage adjusted to shift the laser frequency downward by 5 GHz. This procedure avoids sweeping the laser frequency through the remaining two lines at higher frequency.

Figure 3 shows the observed FID heterodyne beat signals for different values of the initial laser frequency  $\Omega$  or  $\delta \equiv \omega_{21} - \Omega$ , where  $\omega_{21}$  is the frequency of one of the transitions of the low-frequency pair. The numerical solutions of Eq. (4) are shown in Fig. 4, where for the Na D<sub>1</sub> line  $(\Omega - \Omega')/2\pi = 5$  GHz,  $\sigma = 5.8$  GHz,  $\Gamma = 1.6$  GHz,  $\chi = 2.3$  GHz,  $\chi = 32$  ns, and  $\chi = 0.019$ . The laser power density is 3 W/cm<sup>2</sup> ( $\chi = 0.055$ ), and 5% of the beam is absorbed in a 10-cm path of Na at a pressure of  $\chi = 32$  Note that the large frequency switch makes it possible for the first time to switch completely outside the Doppler linewidth, which is 0.77 GHz for Na.

As shown in Fig. 3, first-order FID and nonlinear FID can be distinguished by varying the preparative laser frequency  $\Omega$ . This is because the intensity of nonlinear FID depends on the optical dipole induced in a *single velocity group*. Since the density of any given velocity group is a Gaussian exp  $[-(\delta/\sigma)^2]$ , the nonlinear FID signal will decrease rapidly with laser detuning [see Eq. (6)]. First-order FID, however, is primarily a nonresonant phenomenon in which all velocity groups participate weakly. Examining Eq. (8), one can see that the first-order FID varies slowly with laser tuning  $\delta$ . By tuning off resonance, therefore, one should see a slow reduction in first-order FID and a rapid disappearance of nonlinear FID.

A more physical explanation of the frequency dependence of first-order FID is that it behaves like the dispersive part of a Lorentzian lineshape in which Doppler broadening has been ignored. For example, a Lorentzian  $(\gamma + ix)/(\Delta^2 + x^2)$  approaches i/x at large detuning and yields the slow tuning behavior described above. For small detuning, we also expect the first-order FID signal to change sign as we pass through resonance, and furthermore to equal zero exactly at resonance. These characteristics are evident in Figs. 3 and 4.

Figure 3(a) shows the observed FID signal for the laser tuned 1.5 GHz below the transition frequency  $(\delta/2\pi=1.5~{\rm GHz})$ . The nonlinear FID is reduced by a factor of  $e^2$  and does not appear. The observed decay is obviously nonexponential and is completed in 500 ps as expected since  $T_2^*$  is 340 ps. A careful analysis shows that the beat frequency is  $\approx 6.5~{\rm GHz}$ , which is equal to  $(\omega_{21}-\Omega')/2\pi$  rather than  $(\Omega-\Omega')/2\pi=5~{\rm GHz}$ .

Figure 3(b) shows the FID for  $\delta/2\pi=0.7$  GHz. Here there is a large amplitude preparation due to the saturation of a resonant velocity group. The decay, which persists beyond the first-order FID, is exponential in agreement with Eq. (6), being given by  $\exp{(-\chi t)}$  in this power-broadened regime with  $\chi=0.8$  GHz. The observed beat frequency is equal to the laser frequency switch of 5 GHz. These signals are also absorptive since their phase is invariant to laser tuning.

Figure 3(c) shows the FID for  $\omega_{21} - \Omega = 0$ . Note that here the first-order and nonlinear FID cancel at the time origin, and the decay of the first-order term manifests itself as a Gaussian build-up of the nonlinear FID. The corresponding theoretical result in Fig. 4(c) for  $\delta = 0$  shows this interference effect again but in a more dramatic way since  $\chi = 2.3$  GHz.

In Fig. 3(d),  $\delta/2\pi = -1$  GHz and we see that tuning the laser from the low to the high frequency side of the transition reverses the phase of the first-order FID. Compare the theoretical curves of Figs. 4(b) and 4(d), where  $\delta/2\pi = 1$  and -1 GHz, respectively, which show the same phase reversal.

Figure 3(d) also gives evidence of a hyperfine interference beat because the laser is now tuned midway between the two pairs of lines so that all four transitions are prepared. The FID is now modulated at ≈1.8 GHz, which is the ground state hyperfine splitting of Na. The mechanism for this process is very likely a coherent Raman beat effect [15], but further studies are needed in testing this idea. In any event, it now becomes possible to detect microwave splittings by a transient method where the beat frequency exceeds quantum beat [16] measurements by at least one order of magnitude.

#### Summary

We have described a laser frequency switching technique that permits coherent optical transient investigations on a subnanosecond time scale. A key feature of these measurements is that they are highly reproducible and lend themselves to quantitative analysis. This point is illustrated by optical FID, which shows new characteristics when the temporal resolution is  $\approx 100$  ps. Detailed theoretical predictions of these new coherence effects are

faithfully observed. It is evident that other coherent transients can be observed in this way where the time scale may be reduced even further.

#### **Acknowledgments**

The technical assistance of D. E. Horne and K. L. Foster proved most valuable and is acknowledged with pleasure. This work was supported in part by the U.S. Office of Naval Research, Washington, DC, under Contract No. N00014-78-C-0246.

#### References

- 1. R. G. DeVoe and R. G. Brewer, *Phys. Rev. Lett.* 40, 862 (1978)
- R. G. Brewer and A. Z. Genack, Phys. Rev. Lett. 36, 959 (1976); A. Z. Genack and R. G. Brewer, Phys. Rev. A 17, 1463 (1978).
- 3. R. G. DeVoe and R. G. Brewer (submitted to Phys. Rev.).
- 4. R. G. Brewer and R. L. Shoemaker, *Phys. Rev. A* 6, 2001 (1972)
- F. A. Hopf, R. F. Shea, and M. O. Scully, *Phys. Rev. A* 7, 2105 (1973).
- K. L. Foster, S. Stenholm, and R. G. Brewer, *Phys. Rev. A* 10, 2318 (1974).
- 7. Handbook of Mathematical Functions, National Bureau of Standards Applied Mathematics Series 55, M. Abramowitz and I. A. Stegun, Eds., U.S. Government Printing Office, Washington, DC, 1964, p. 297.
- P. F. Liao, J. E. Bjorkholm, and J. P. Gordon, *Phys. Rev. Lett.* 39, 15 (1977).
- R. G. Brewer, in Frontiers in Laser Spectroscopy, R. Balian, S. Haroche, and S. Liberman, Eds., North-Holland Publishing Co., New York, 1977, p. 341.
- 10. E. L. Hahn, Phys. Rev. 77, 297 (1950).
- W. W. Rigrod and I. P. Kaminow, Proc. IEEE 51, 137 (1963); I. P. Kaminow, Phys. Rev. Lett. 6, 528 (1961).
- 12. An Introduction to Electrooptic Devices, I. P. Kaminow, Ed., Academic Press, Inc., New York, 1974: (a) pp. 213-237; (b) p. 182; (c) p. 92, Eq. (10).
- 13. H. Kogelnik and T. Li, Proc. IEEE 54, 1312 (1966).
- 14. See for example R. C. Eden, Proc. IEEE 63, 32 (1975).
- R. L. Shoemaker and R. G. Brewer, *Phys. Rev. Lett.* 28, 1430 (1972); R. G. Brewer and E. L. Hahn, *Phys. Rev. A* 8, 464 (1973); *Phys. Rev. A* 11, 1641 (1975).
- S. Haroche, in High Resolution Laser Spectroscopy, K. Shimoda, Ed., Springer-Verlag, Berlin, 1977, p. 253.

Received March 1, 1979

The authors are located at the IBM Research Division laboratory, 5600 Cottle Road, San Jose, California 95193.